Improving the stability and accuracy of population balance numerical solutions: I- methods of describing drop size distribution

G. Polprasert, A.M. AlTaweel, J. Webber and P. Gupta
Chemical Engineering Dept., Dalhousie University, Halifax, NS B3J 2X4, Canada
A.S.I. Elsayed
Eng. Mathematics and Physics Dept., Alexandria University, Alexandria 21544, Egypt

The method most commonly used for simulating dispersed phase systems is the population balance technique by itself or in conjunction with CFD. Unfortunately, the accuracy of this technique has rarely been investigated and the computational effort associated with its use renders its integration into CFD code very cumbersome. One of the errors encountered in solving Population Balance [PB] simulations is that resulting from the numerical solution of the integro-differential PB equations. One of the major factors affecting the stability and accuracy of the resulting numerical solution is the method used to describe the drop size distributions encountered in the system. Most investigators use a limited number of fixed drop size intervals and the drops present within that interval are represented by an appropriately selected class average (arithmetic, geometric or logarithmic mean). Significant errors are introduced through the use of classes and the inappropriate selection of the average value representing a class. Reasonably stable and accurate numerical solutions were obtained by using optimal number of classes in the drop size domain (10 to 200 classes). However, this improvement requires excessively large computational effort, particularly when low residual errors are required. However, highly accurate and rapid numerical solutions were obtained when the drop size distribution is described as a continuous function that is sampled at regular interval. In this case, numerical integration over a selected section of the drop size domain is used to calculate breakage and coalescence rates at different drop sizes.

من مزايا نموذج الاتزان العددي: ١- مبني على مبدأ بقاء الكتلة. ٢- يمكن أن يستخدم لحساب توزيع حجم جزيئات الطور المنتشر وحساب التغير في درجات الحرارة ودرجة التركيز داخل كل حجم. ٣- يأخذ في الاعتبار عملات انتقال الحرارة والكتلة بالإضافة إلى مدى التفاعل. ٤- يأخذ في الاعتبار عمليات الخلط والانتشار. ولكن لم يستخدم نموذج الاتزان العددي عمليا في الصناعة بشكل كبير نظر للأخطاء في النتائج التي تنشأ من: ١- عدم استخدام التمثيل الصحيح لمعدل استنفاذ الطاقة. ٢- فرض أن عمليات التكسر والالتحام للقطرات ثنائية. ٣- أخطاء تنشأ من الحل العددي نظرا لعدم توفر المعلومات الكافية عن العوامل التي تؤثر على دقة الحل العددي لنموذج الاتزان العددي. ٤- وجود عدد كبير من النماذج التي تصف عمليات التكسر والالتحام وغالبا يحدث فيها تعارض. يقوم هذا البحث على استكمال دراسة العوامل التي تؤثر على صحة النتائج المستخرجة من حل نموذج الاتزان العددي. أحد أهم الأخطاء التي تنشأ عند حل نموذج الاتزان العددي تنشأ من الحل العددي. وأهم هذه العوامل التي تؤثر في دقة واتزان الحل العددي هي الطريقة المستخدمة لوصف توزيع حجم القطرات في النظام. معظم الباحثين استخدموا عدد محدود من فترات حجم القطرات، بالإضافة إلى تمثيل القطرات الموجودة داخل كل فترة باستخدام متوسط حسابي أو هندسي أو لوغاريتمي. وينشأ خطأ كبير عند استخدام فترات واختيار متوسط غير مناسب لتمثيل كل فترة. وعند استخدام العدد الأمثل من الفترات يمكن على حل عددي دقيق ومتزن بشكل مرضي، ولكن هذا يتطلب مجهود حسابات كبير و خصوصا إذا كان الخطأ المراد صغير. وقد تم الحصول على حل عددي دقيق جدا وسريع عندما وصفنا توزيع حجم القطرات كدالة متصلة واستخدام نظام التمثيل باستخدام نقاط على المنحنى الممثل للدالة.

1. Introduction

The Population Balance Equation [PBE] is the most effective fundamental tool for describing multiphase systems, and has been used to describe multi-phase operations such as crystallization; grinding, inter-phase heat

and mass transfer operations, multi-phase reactions, and flotation.

The advantages of PBE are, (i) it is based on the principles of conservation of mass and physically consistent phenomena, (ii) it can be used to calculate dispersed phase size distribution, and the variation of temperature and concentration within the various sizes, (iii)it can account for heat and mass transfer as well as the extent of reaction, (iv)can account for back mixing, convection, and diffusion, (v)a significant advantage of the PBE is that a vehicle is provided to include the details of the drop/bubble breakage and coalescence processes in terms of the physical parameters and conditions of operation, fig. 1. However, the PBE has not been extensively used by industry because of insensitivity to model assumptions and gross modeling simplifications.

Sovova [1], and Rod and Misek [2] derived exact solution for the PBE in a batch mixer, assuming simple power functions in drop size for breakage and coalescence. Generally, PBE requires numerical solution. Lee et al. [3] applied the population balance equation coupled with the proposed breakage kernel and the previously developed breakage model to the analysis of bubble size distribution for non-coalescing systems in a bench-scale airlift column. They solved the steady-state population balance equation using Simpson's

integration technique. Niyogi et al. [4] solved the population balance equation numerically using adaptive fourth-order Runge-Kutta method. Chatzi et al. [5] described the steady-state drop size distribution in a batch stirred vessel by PBE. They solved PBE using composite Simpson's rule.

The objective of the present work is to develop a user friendly population balance program capable of accurately simulating multi-phase contactors, accurate numerical solution, better representation of the hydrodynamics of industrial units, and having modeling flexibility for various sub-components.

2. PBE formulation

In a dispersed phase system, the material domain comprises a continuous phase and a dispersed phase, the latter as a population of particles (drops, bubbles, or solid) in which the identities of individuals are continually de-stroyed and recreated by breakup and coales-cence processes. Considering the control volume in fig. 2. The population balance model is based on an equation for the continuity of particle numbers in a dispersed phase and is developed from the general conservation equation.
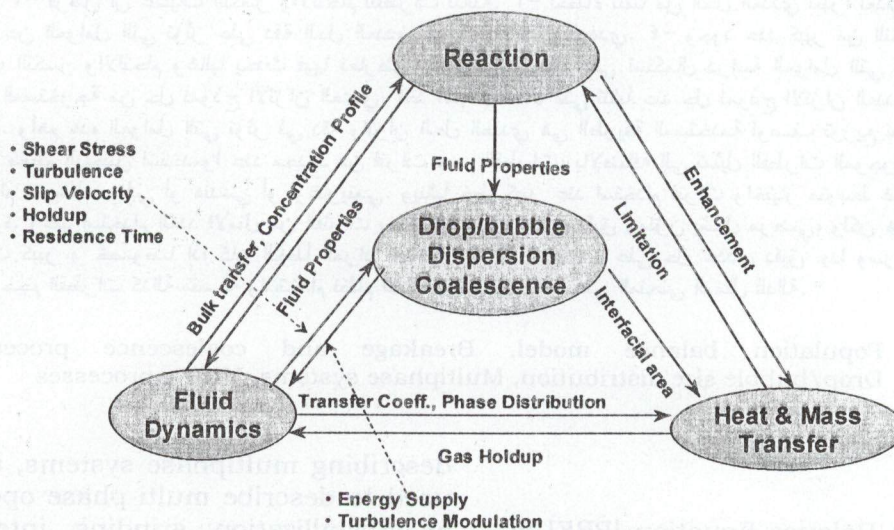

Fig. 1. Role of breakage and coalescence in multi-phase systems.

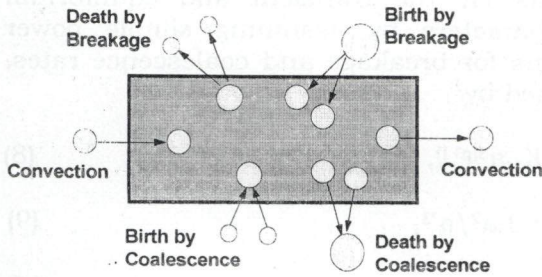Accumulation rate = Flux in (convection & diffusion)–Flux out+ Net generation rate.   (1)

Fig. 2. Control volume.

Consider the distribution of entities $n(r, \xi_1, \xi_2,..., \xi_m, t)$ or the population of particles of the dispersed phase at position r, where r represents the spatial coordinates or "external coordinates", t is the time, and ξ_i represents the i th other property of the entity. ξ_i is also called the internal coordinate and used to give a quantitative description of the state of an individual particle, such as its mass, concentration, temperature, age, volume, etc. In addition to time, there are (3+m) independent variables involved that can be thought of as a (3+m) dimensional space.

The PBE in its most general form [6]

$$\frac{\partial n}{\partial t} \cdot \nabla \bullet (\bar{v}\, n) - B + D = 0. \qquad (2)$$

Where $\bar{V}$ is the coordinate velocity in phase space. For well mixed batch mixing tank, fig. 3, with no reaction or heat/mass transfer, the problem simplifies to the following two dimensional situation [7]

$$\frac{d\,[N(t)\,f(a,t)]}{d\,t} = B_B(a,t) - D_B(a,t) + B_C(a,t) - D_C(a,t). \qquad (3)$$

Where: N(t) is the total number of particles at time t, f(a,t) is the fraction of particles have diameter between a and a+Δa, and $B_B(a,t)$, $D_B(a,t)$, $B_C(a,t)$, and $D_C(a,t)$ are the birth rate by breakage, death rate by breakage, birth rate by coalescence, and death rate by

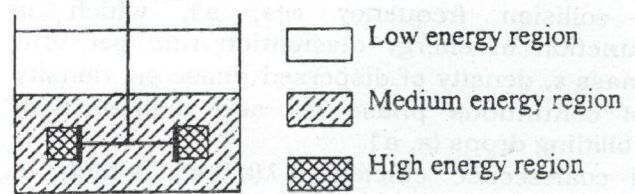coalescence, of particles of diameter a at time t, respectively.

Fig. 3. Batch mixer (agitated tank).

3. Breakage rate

Breakage results in both "death" as well as "birth" within a certain drop size range.

$$B_B(a,t) = \int_a^{a_{max}} \beta(a,a')\, \varsigma(a')\, \Omega(a')\, N(t)\, f(a',t)\, da' \qquad (4)$$

$$D_B(a,t) = \Omega(a)\, N(t)\, f(a,t). \qquad (5)$$

From eqs. (4, 5), the breakage rate is affected by [8]:

i- breakage frequency $\Omega(a)$, which is function of energy dissipation rate per unit mass ε, surface tension σ, density of dispersed phase ρ_D, density of continuous phase ρ_C, viscosity of dispersed phase μ_D, and viscosity of continuous phase μ_C.

ii- number of daughter drops $\varsigma(a)$, where $\varsigma(a')$ may be (2,3,4,...).

iii- size distribution of daughter drops $\beta(a,a')$, where $\beta(a,a')$ is assumed (equi-sized, Normal, Gamma, Beta,...).

4. Coalescence rate

Coalescence results in both "death" as well as "birth" within a certain drop size range.

$$B_C(a,t) = \int_0^{a/2} \lambda(a-a',\, a')\, \omega(a-a',\, a')\, N(t) f(a-a',t)\, N(t)\, f(a',t)\, da \qquad (6)$$

$$D_C(a,t) = N(t)\, f(a,t) \int_0^{a_{max}-a} \lambda(a,\, a')\, \omega(a,\, a')\, N(t)\, f(a',t)\, da. \qquad (7)$$

Here: $\lambda(a,\, a')$ is the coalescence efficiency between drops of size a and a', and $\omega(a,\, a')$ is the collision frequency between drops of size a

and a'. From eqs. (6,7), the coalescence rate is affected by [8]:

i- collision frequency $\omega(a, a')$, which is function in energy dissipation rate per unit mass ε, density of dispersed phase ρ_D, density of continuous phase ρ_C, and diameters of colliding drops (a, a').

ii- coalescence efficiency $\lambda(a, a')$, which is defined as the fraction of collisions between drops of diameter a and a' that result in coalescence. It is function of contact time between drops and coalescence time which is the time required for drops to coalesce.

5. Errors in population balance simulation

5.1. Formulation errors

Formulation errors are due to:

i-disregard of the large spatial variation in energy dissipation rate (ε).

ii-emphasis on binary breakage and coalescence.

iii-presence of large numbers of models describing the various sub-processes (often conflicting).

iv-lack of experimental data in which coalescence or breakage mechanisms dominate (to discriminate amongst the various sub-processes).

v-lack of information on the factors affecting the accuracy of numerical solutions.

5.2. Solution errors

The sources of error in numerical solutions are:

i-discretization errors in time and drop size domain,

ii-truncation errors, due to approximating exact mathematical procedures,

iii-round off error, due to inexact representation of floating point numbers,

iv-propagated errors, due to errors from previous steps carried through to succeeding steps, and

v-the underestimation or overestimation to the time of equilibrium state between breakage and coalescence processes.

6. The Rod and Misek analytical solution

Rod and Misek [2] obtained analytical solutions for the transient and equilibrium drop diameters by assuming simple power functions for breakage and coalescence rates, expressed by:

$$\Omega(a') = K_s \, a^{3(p+1)}, \tag{8}$$

$$\beta(a,a') = 3 \, a^2/a'^3, \tag{9}$$

$$\varsigma(a') = 2, \tag{10}$$

$$\lambda(a-a', a') \, \omega(a-a', a') = K_c \, (a^3 + a'^3)^p . \tag{11}$$

Where K_s and K_c are the breakage and coalescence rate constants. The analytical solution of the steady-state PBE using the above models, leads to the steady-state drop number density:

$$f(a) = \frac{3 \, a^2}{\bar{a}^3} \exp\left[-\left(\frac{a}{\bar{a}}\right)^3\right]. \tag{12}$$

Mean volume drop diameter $\bar{a}$, as the parameter of the distribution, is given by:

$$\bar{a} = \left(\frac{3}{\pi} \frac{K_c \, \phi}{K_s}\right)^{1/6} . \tag{13}$$

Where ϕ is the volume fraction of the dispersed phase. The transient distribution developing during the transition from one steady state, characterized by the mean volume diameter $\bar{a}_o$ to another steady state, characterized by the mean volume diameter $\bar{a}_\infty$, can be described by:

$$f(a,t) = \frac{3 \, a^2}{[\bar{a}(t)]^3} \exp\left[-(a/\bar{a}(t))^3\right]. \tag{14}$$

The time variation of the value $\bar{a}$, depending on the exponent p, is described by differential equation,

$$\frac{d \bar{a}}{dt} = \frac{\Gamma(p+2)}{3} K_s \, \bar{a}^{3p-2} \, (\bar{a}_\infty^{\,6} - \bar{a}^{\,6}) . \tag{15}$$

The solution of eq. (15), for p=0, has the form:

$$\bar{a}(t) = \bar{a}_\infty \left(\frac{1 + A \exp(- 2 K_s \ \bar{a}_\infty^3 t)}{1 - A \exp(- 2 K_s \ \bar{a}_\infty^3 t)} \right)^{1/3}, \quad (16)$$

where;

$$A = \frac{\bar{a}_o^3 - \bar{a}_\infty^3}{\bar{a}_o^3 + \bar{a}_\infty^3}. \quad (17)$$

The analytical solution of Rod and Misek [2] was used to identify the factors controlling the accuracy of numerical solutions and develop algorithms that can minimize them. The rate at which equilibrium is achieved depends on the value of the coalescence and breakage rate constant (K_c & K_s).

Fig. 4 shows the effect of sudden variation in the RPM of the impeller, on the volume mean diameter in the batch mixer.

7. Discretization of drop size distribution

The Drop Size Distribution (DSD) is descretized into drop size classes, fig. 5. The arithmetic mean diameter usually used to describe the class. The number of classes used to describe DSD as low as 7. No clear rules exist for the drop size range over which calculations should be conducted.
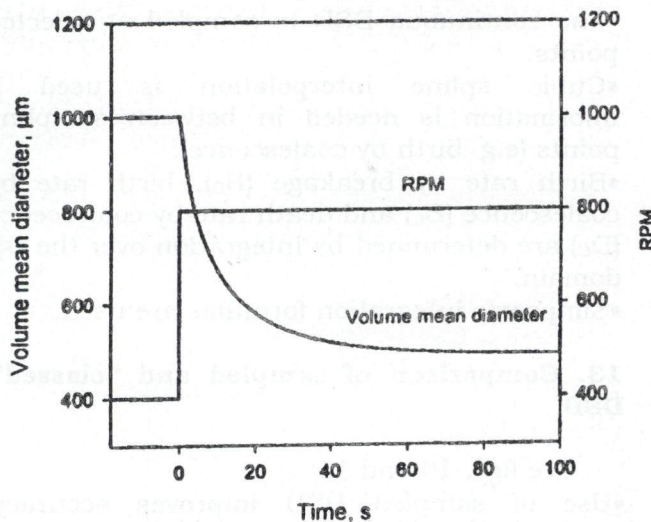
8. Use of DSD classes in PBE

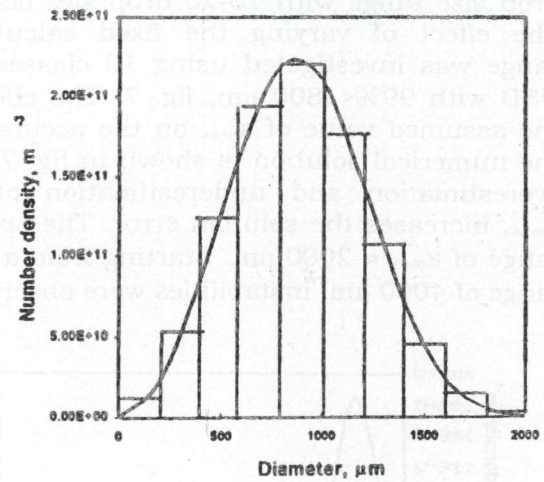At a particular drop size a_i, fig. 6:

Fig. 5. Discretization of DSD.

• calculate birth rate by breakage (B_B), by summation of birth rates resulting from disintegration of larger drop sizes,
• calculate death rate by breakage (D_B), at the class represented by a_i,
• calculate birth rate by coalescence (B_C), by summation of birth rates resulting from the coalescence of small drop sizes, and
• calculate death rate by coalescence (D_C), by summation of death rates resulting from the formation of larger drops by coalescence with all other drop classes.
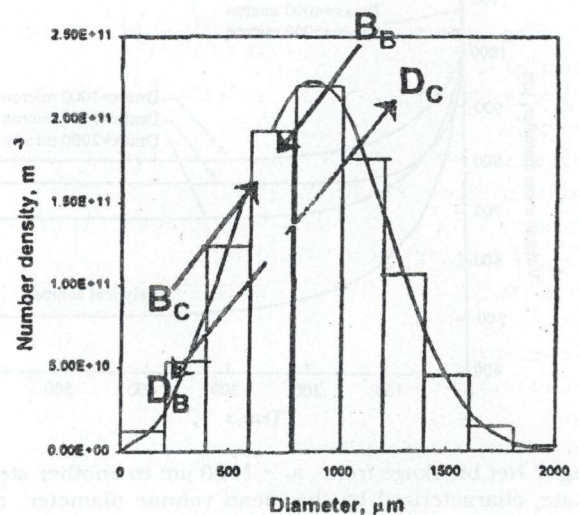

Fig. 4. Effect of RPM on volume mean diameter.

Fig. 6. Net generation rate at particular drop size.

9. Size of the drop size domain

Most investigators used a fixed maximum drop size range with 10-20 drop size classes. The effect of varying the fixed calculation range was investigated using 10 classes and DSD with 99%<1800 μm, fig. 7. The effect of the assumed value of a_{max} on the accuracy of the numerical solution is shown in fig. 7. The overestimation and underestimation of the a_{max}, increases the solution error. The optimal range of $a_{max} \approx 2000$ μm. Starting from a DSD range of 4000 μm, instabilities were observed.
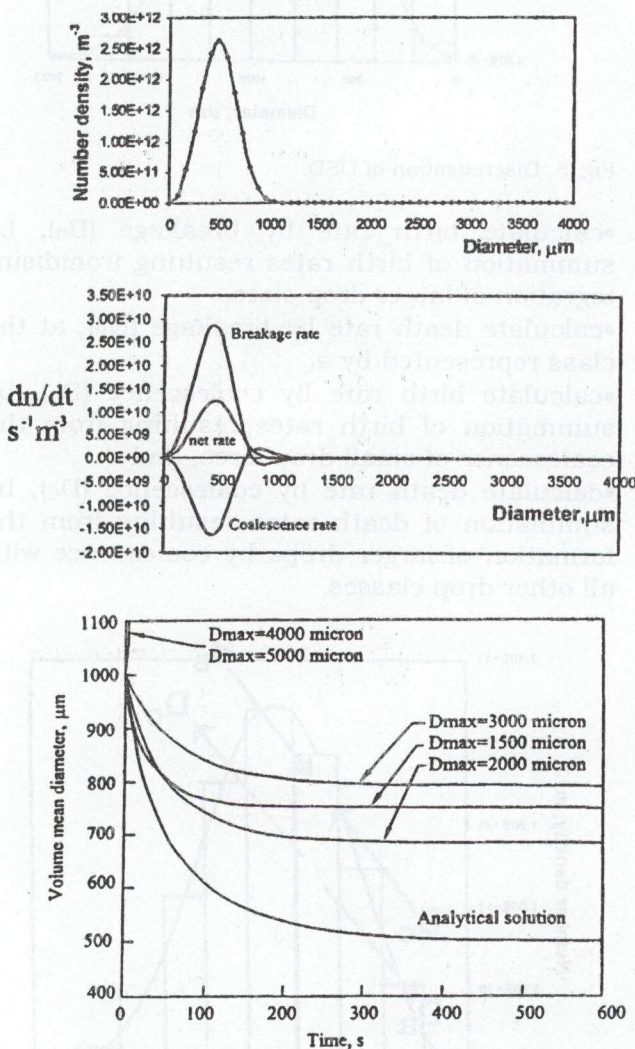
Fig. 7 Net breakage from $\bar{a}_o = 1000$ μm to another steady state, characterized by the mean volume diameter $\bar{a}_\infty = 500$ μm. Fixed time step size, 1000 time intervals.

10. The need to limit the size of the DSD

In the region where the net rate of change is very small, fig. 8, truncation error was found to play a significant role. This is caused by the net rate of change being the difference between two large drop-birth and drop-death rates.

11. Adaptive integration range

Limit the integration range in the drop size domain to values that do not exhibit instabilities:
• At each time interval, limit the integration range at the drop size where the netrate of change is less than 0.01% of the maximum net rate, or
• At each time interval, limit the integration range at the drop size where the number density is less than 0.001% of the maximum number density (>99.99% mass conservation).
• Relative error was reduced from 17.6 to 10.7% (at 36s) when 10 drop size intervals and classed DSD were initially used (fixed interval size in the DS domain).
• As a result of the decreasing a_{max} value, the number of sampling intervals used to describe the DSD decreased. This leads to enhancing the error.

12. Use of sampled DSD in PBE

In this approach, fig. 9:
• The continuous DSD is sampled at selected points.
• Cubic spline interpolation is used if information is needed in between sampling points (e.g. birth by coalescence).
• Birth rate by breakage (B_B), birth rate by coalescence (B_C) and death rate by coalescence (D_C) are determined by integration over the DS domain.
• Simpson's integration formulae are used.

13. Comparison of sampled and "classed" DSD

See figs. 10 and 11:
• Use of sampled DSD improves accuracy (reduces error from 17.9 to 5.4% at 36s).

- Instability caused by other sources of error such as, fig. 10:
- Only 50 fixed time steps,
- 10 drop size intervals, and
- A fixed DSD range was used in drop size domain calculations.

- Both solutions are stable, fig. 11, if 1000 fixed time steps are used instead of 50, and accuracy was improved (%error was reduced from 17.6 to 1.64% at 36s).
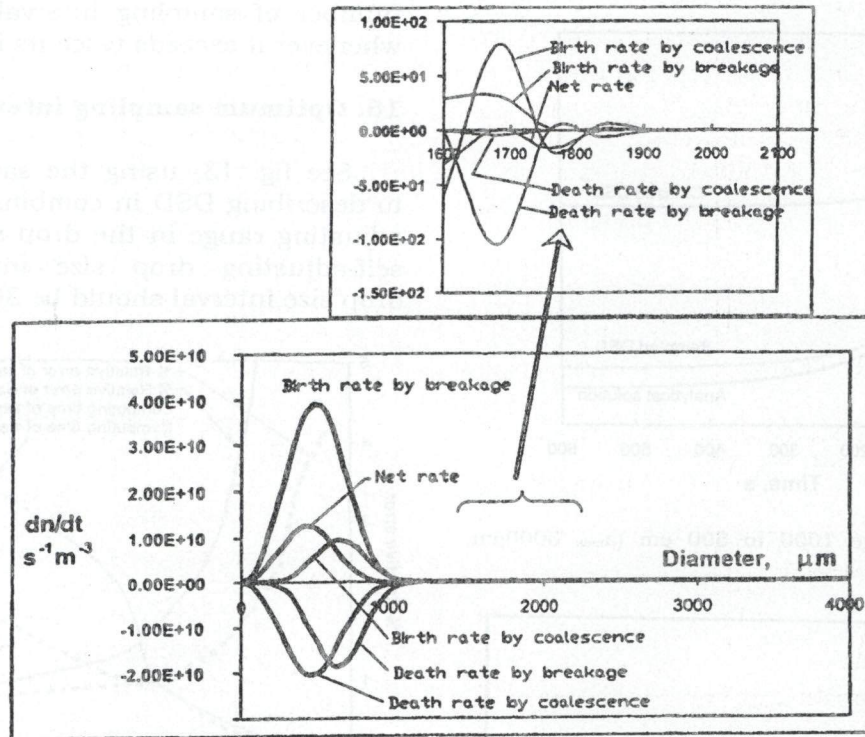

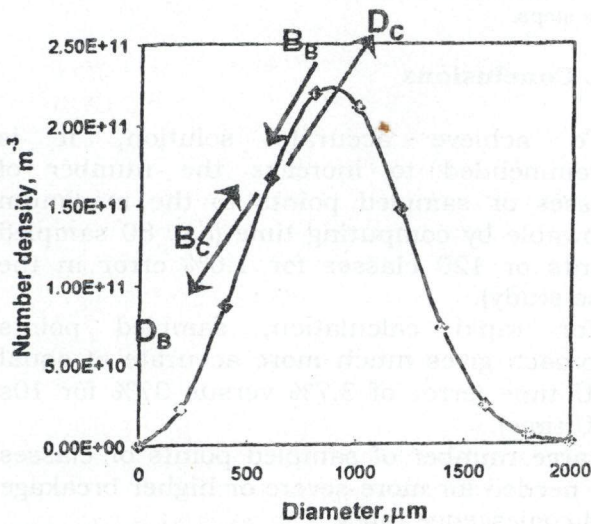Fig. 8. Region of small net rate of change.
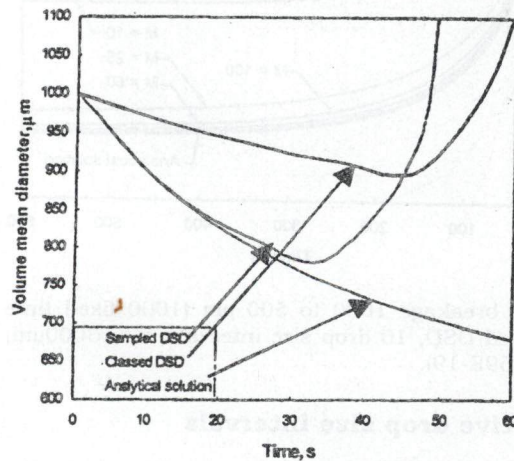

Fig. 9. Sampled drop size distribution.

Fig. 10 Net breakage 1000 to 500 µm (a_{max} 3000µm, ks/kc=1.6369E-19).

14. Number of drop size classes

See fig. 12; increasing the number of drop size classes results in increasing accuracy. However, computational time is significantly increased 1.6-fold (from 10 to 25 classes), and 8.7-fold (from 10 to 100 classes).
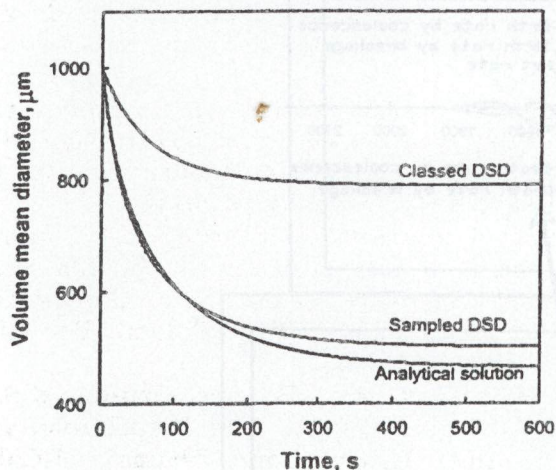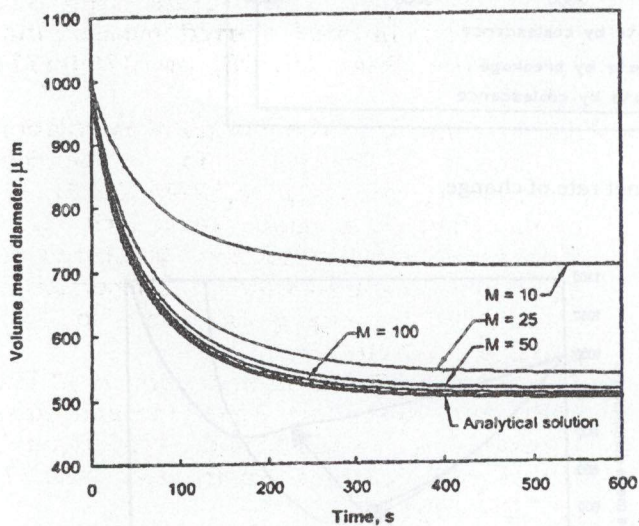

Fig. 11 Net breakage 1000 to 500 μm (a_{max} 3000μm, ks/kc=1.6369E-19).

Fig. 12 Net breakage 1000 to 500 μm (1000 fixed time steps, classed DSD, 10 drop size intervals, a_{max} 3000μm, ks/kc=1.6369E-19).

15. Adaptive drop size intervals

The number of sampling intervals need to be maintained at a suitable value to enhance accuracy without excessive computational effort:

• In the case of net breakage processes, the number of sampling intervals is doubled whenever it decreases below 50% of its initial value (using cubic spline interpolation).

• In the case of net coalescence processes, the number of sampling intervals is cut by half whenever it exceeds twice its initial value.

16. Optimum sampling intervals

See fig. 13; using the sampling approach to describing DSD in combination with a self-adjusting range in the drop size domain, and self-adjusting drop size interval, optimum drop size interval should be 30-80.
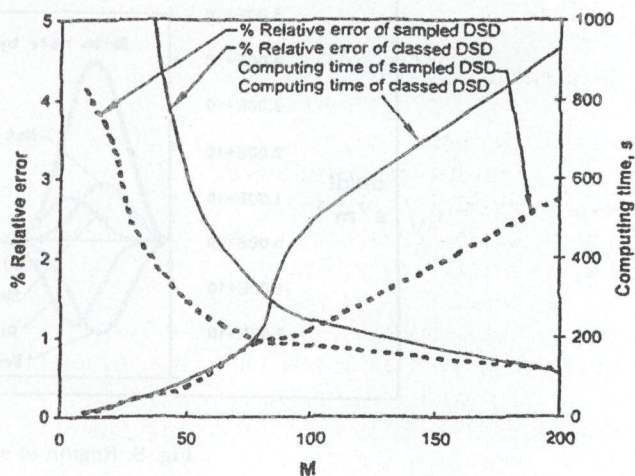

Fig. 13 Net breakage from 1000 to 500 μm, and 1000 fixed time steps.

17. Conclusions

1-To achieve accurate solution, it is recommended to increase the number of classes or sampled points to the maximum allowable by computing time (e.g. 80 sampled points or 120 classes for 1.0% error in the case study).

2-For rapid calculation, sampled points approach gives much more accurate at equal CPU time (error of 3.7% versus 37% for 10s CPU time).

3-Large number of sampled points or classes are needed for more severe or higher breakage and coalescence rates.

4-Using an adjustable integration range in the drop size domain enhances the stability and accuracy of PBE solutions.

5-Optimal number of sampling points appears to be 30-80 points.

6-An algorithm for maintaining the number of sampling point within their optimal range, as the drop size range increases or decrease, was developed.

7-The error resulting from numerically solving PBE can be as low as 0.10% by using the above mentioned features in combination with other approaches that address the remaining sources of error.

Nomenclature

a, a'	diameter of drop,
$\bar{a}$	volume mean diameter of drop,
a_{max}	maximum drop size,
K_C	coalescence coefficient,
K_S	break-up coefficient,
t	time,
$N(t)$	the total number of particles at time t,
$f(a,t)$	the fraction of particles have diameter between a and $a+\Delta a$,
$B_B(a,t)$	birth rate by breakage, of particles of diameter a at time t,
$D_B(a,t)$	death rate by breakage, of particles of diameter a at time t,
$B_C(a,t)$	birth rate by coalescence, of particles of diameter a at time t,
$D_C(a,t)$	death rate by coalescence, of particles of diameter a at time t,
$\varsigma(a')$	number of drops formed per breakage of drop of size a',
$\beta(a,a')$	number fraction of droplets with size a' formed by breakage of drop of size a,
$\Omega(a')$	breakage frequency of drop of size a',
$\lambda(a, a')$	coalescence efficiency of drops of size a with drops of size a',
$\omega(a, a')$	collision frequency between drops of sizes a and a', and
ϕ	volume fraction of the dispersed phase.

References

[1] Sovova, H., "Drop Size Distributions by Power Functions of Breakage and Coalescence", Collection Czechoslovak Chem. Commun. Vol. 47, pp. 2393-2402 (1982).

[2] Rod, V. and Misek, T., "Stochastic Modelling of Dispersion Formation in Agitated Liquid-Liquid Systems", Trans. IchemE, Vol. 60, pp. 48-53 (1982).

[3] Lee, Chung-Hur, Erickson, L.E., and Glasgow, L.A., "Dynamics of Bubble Size Distribution in Turbulent Gas-Liquid Dispersions", Chem. Eng. Comm., Vol. 61, pp. 181-195 (1987).

[4] Niyogi, D., Kumar, R., and Gandhi, K.S., "Modelling of Bubble Size Distribution in Free Rise Polyurethane Foams", AIChE Journal, Vol. 38 (8), pp. 1170-1184 (1992).

[5] Chatzi, E.G., Gavrielides, A.D., and Kiparissides, C., "Generalized Model for Prediction of the Steady-State Drop Size Distributions in Batch Stirred Vessels", Ind. Eng. Chem. Res. Vol. 28, pp. 1704-1711 (1989).

[6] Ramkrishna, D., "The Status of Population Balances", Reviews in Chemical Engineering, Vol. 3 (1), pp. 49-95 (1985).

[7] Coulaloglou, C.A. and Tavlarides, L.L., "Description of Interaction Processes in Agitated Liquid-Liquid Dispersions", Chemical Engineering Science, Vol. 32, pp. 1289-1297 (1977).

[8] Tavlarides, L.L. and Stamatoudis, M., " The Analysis of Interphase Reactions and Mass Transfer in Liquid-Liquid Dispersions", Advances in Chemical Engineering, Vol. 11, pp. 199-273 (1981).